# Can we detect local helioseismic parameter shifts in coronal holes?



2013 J. Phys.: Conf. Ser. 440 012019

(http://iopscience.iop.org/1742-6596/440/1/012019)

Journal of Physics: Conference Series **440** (2013) 012019 doi:10.1088/1742-6596/440/1/012019

# Can we detect local helioseismic parameter shifts in coronal holes?

**R Howe[1], D A Haber[2], R S Bogart[3], S Zharkov[4,5], D Baker[4], L Harra[4] and L van Driel-Gesztelyi[4]**

[1]School of Physics and Astronomy, University of Birmingham, UK
[2]University of Colorado, Boulder, CO, USA
[3]Stanford University, USA
[4]UCL/MSSL, United Kingdom
[5]Department of Physics and Mathematics, University of Hull, UK

E-mail: rhowe@nso.edu

**Abstract.** Changes in helioseismic mode parameters in active regions and across the solar disk are well documented, but local magnetic activity and geometric effects may not account for all of the scatter seen in the results. We use results from the *Helioseismic and Magnetic Imager* ring-diagram pipeline for Carrington rotation 2113 to look for differences in mode amplitude and frequency between coronal holes and other quiet-Sun regions. While we do not find a systematic difference, the results do suggest that the correlation between magnetic activity index and mode parameters shows less scatter in coronal hole regions than in general quiet Sun.

## 1. Introduction

Helioseismic mode parameters in the five-minute frequency range have long been known to correlate (frequency, linewidth) and anticorrelate (amplitude) with surface magnetic activity indices at a wide range of scales. However, the indices do not account for all of the variation and scatter. Here we investigate the possible contribution from coronal holes effects to the local mode properties.

## 2. Data

### *2.1. Helioseismic Data*

We use ring-diagram parameters (specifically mode frequency and the logarithmic mode amplitude) from the *Helioseismic and Magnetic Imager* (HMI) ring diagram pipeline [1] for 5-degree tiles. These tiles, each tracked at the Carrington rate for an 8-hour period, are processed for the full solar disk using both the "rdfitf" [2] (symmetric) and "rdfitc" [3] (asymmetric) peak-fitting algorithms. Each patch has a magnetic activity index [MAI] calculated from the total unsigned magnetic flux in the patch as measured by HMI, averaged across the observing interval. The available data cover Carrington rotations 2096 to 2126, but for this report we concentrate on the rdfitf fits for C.R. 2113, which shows a good mixture of coronal holes and active regions. For the purposes of this analysis, we first correct the mode parameters for disk-position effects by subtracting a disk-position average (excluding patches with magnetic index greater than 10 G) over the whole Carrington rotation from the parameters at each position; we then form a

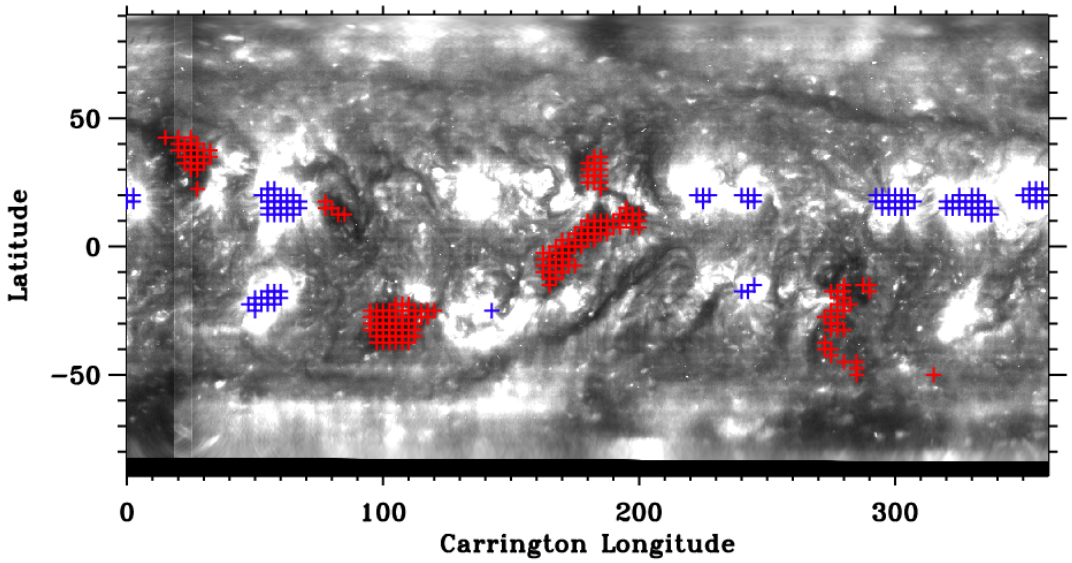


**Figure 1.** The "coronal hole" areas in red and the areas with MAI $\geq 30$ G in blue, superimposed on the EIT 195 Å intensity, for Carrington rotation 2113.

synoptic chart by averaging the parameters for each location in heliographic latitude/longitude across the whole disk passage of the location.

*2.2. Coronal Hole Identification*

The identification of coronal holes is a research topic in itself and beyond the scope of this work. We use the NSO GONG[1] and SOLIS[2] preliminary synoptic maps of open-field regions based on PFSS modeling of synoptic magnetograms, together with EIT synoptic charts[3] of EUV 195 Å intensity, to locate regions that can be considered as coronal holes. We designate a ring-diagram patch as being in a coronal hole if it has an MAI less than 30 G, has non-zero values in either of the two PFSS maps, and has an EIT 195 Å intensity less than the median value for the rotation. Because of projection difficulties with the high-latitude measurements, we concentrate on features within $\pm 50$ deg of the Equator. Figure 1 shows the active (MAI $\geq$ 30 G) and coronal-hole regions superimposed on the EIT 195 Å intensity map for C.R. 2113.

## 3. Results

For illustrative purposes, we select two peaks in the ring-diagram spectrum; $l = 660, n = 1$, which lies close to the center of the five-minute $p$-mode spectrum, and $l = 840, n = 3$, which has a frequency close to the acoustic cutoff. Figures 2 and 3 show synoptic charts of the peak frequency and amplitude for each case over C.R. 2113, and Figure 4 shows scatter plots of the same data as a function of MAI in the quiet-Sun range, with results from the coronal-hole patches indicated by color.

As seen in earlier work [4–7], and in many global-mode studies, for example [8–10], in the five-minute band the tendency is for frequencies to be positively, and amplitudes negatively,

[1] http://gong.nso.edu/data/magmap/
[2] ftp://solis.nso.edu/synoptic/
[3] http://lasco-www.nrl.navy.mil/carr_maps/eit/_synomap/

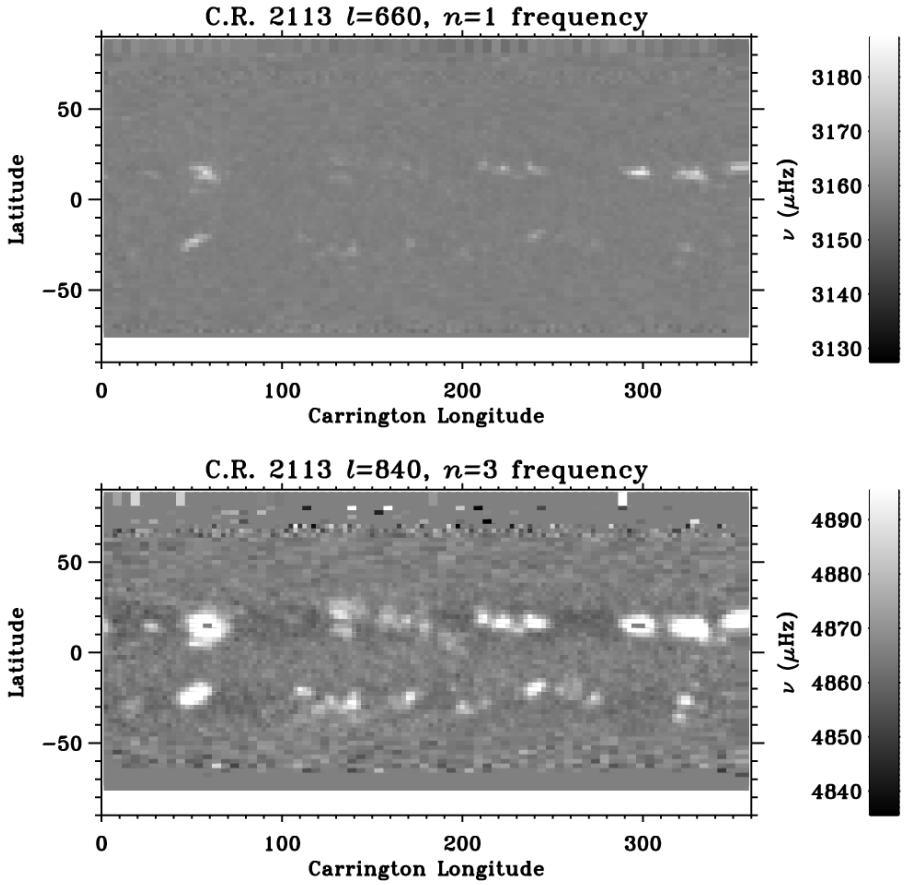


**Figure 2.** Maps of frequency shifts for rdfitf fits to two sample peaks – one (top) in the middle of the 5-min band and one (bottom) close to the acoustic cutoff.

correlated with the magnetic activity index. In the case of mode amplitude, this trend also applies to power maps at the pixel-by-pixel level, *e.g.* [11; 12]. Closer to the acoustic cutoff, while the frequency continues to increase in the range covered by the fits to the 5-degree tiles, the trend in amplitude reverses; detailed examination of power maps reveals a "halo" of enhanced power surrounding an active region. These haloes may arise from the interaction of waves in the solar atmosphere with inclined magnetic fields around active regions. This halo effect is not easily seen in ring-diagram measurements with the conventional 15-degree tiling, but the five-degree tiles give a fine enough spatial resolution to reveal the halo. For the higher-frequency case, therefore, the direct anti-correlation between activity level and amplitude breaks down to some extent and the plots show more scatter. In each case, the coronal-hole data points lie within the "cloud" of general quiet-Sun measurements; however, there does seem to be a tendency for the coronal-hole measurements to be somewhat less scattered.

## 4. Discussion

The five-degree ring-diagram tiles are useful for seeing the fine details of changes to local parameters around active regions, such as the high-frequency haloes. The improved quality of HMI magnetograms compared to those from MDI allows us to look at the effects of relatively weak fields. So far we have found no obvious signature of coronal holes in the frequency and

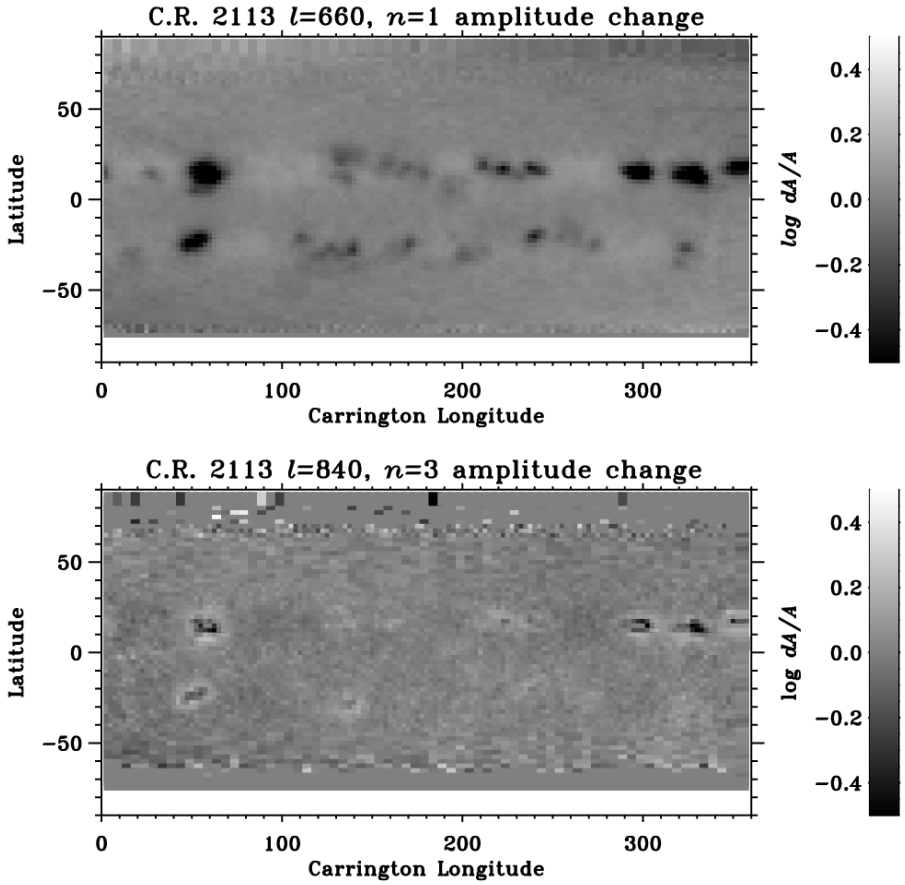


**Figure 3.** Maps of amplitude shifts for rdfitf fits to two sample peaks – one (top) in the middle of the 5-min band and one (bottom) close to the acoustic cutoff.

mode-amplitude parameters. However, the scatter in the coronal hole areas does seem to be marginally smaller than for general quiet Sun. This would make sense in terms of simpler field geometry and less emerging flux in coronal hole regions. In future work we hope to examine this question in more detail using data from many solar rotations.

**Acknowledgments**
RH acknowledges computing support from NSO. We acknowledge the Leverhulme Trust for funding the "Probing the Sun: inside and out" project upon which this research is based. HMI data courtesy of SDO (NASA) and the HMI consortium. This work utilizes GONG and SOLIS data obtained by the NSO Integrated Synoptic Program (NISP), managed by the National Solar Observatory, which is operated by the Association of Universities for Research in Astronomy (AURA), Inc. under a cooperative agreement with the National Science Foundation.

**References**
[1] Bogart R S, Baldner C, Basu S, Haber D A and Rabello-Soares M C 2011 *Journal of Physics Conference Series* **271** 012008
[2] Haber D A, Hindman B W, Toomre J, Bogart R S, Thompson M J and Hill F 2000 *Solar Phys.* **192** 335–350

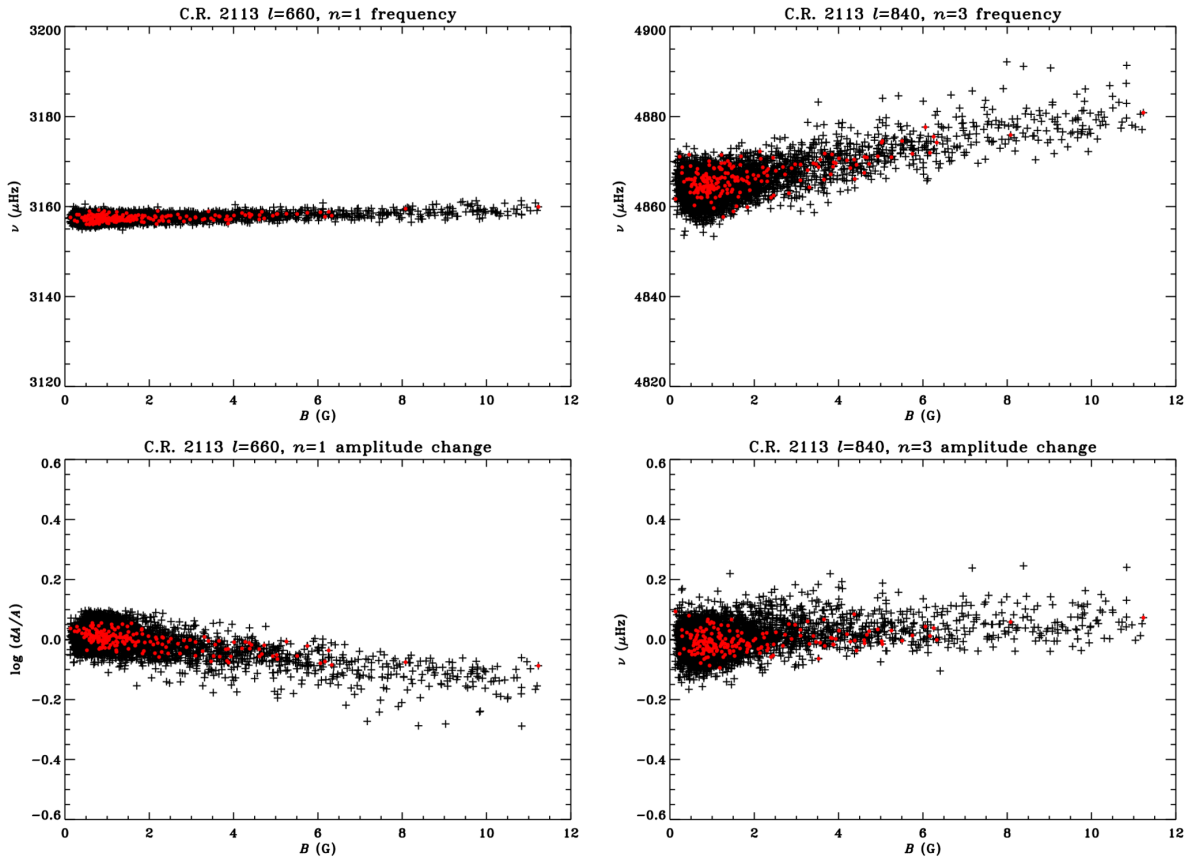


**Figure 4.** Scatter plots of frequency (top) and amplitude (bottom) change against MAI for low-activity regions in C.R. 2113. The red symbols represent patches in the coronal hole areas and the black symbols other patches in the same MAI range, for sample peaks in the 5-min band (left) and at the acoustic cutoff (right). Both sets of data are restricted to latitudes below 50 degrees.

[3] Basu S and Antia H M 1999 *Astrophys. J.* **525** 517–523 (*Preprint* `arXiv:astro-ph/9906252`)

[4] Hindman B, Haber D, Toomre J and Bogart R 2000 *Solar Phys.* **192** 363–372

[5] Rajaguru S P, Basu S and Antia H M 2001 *Astrophys. J.* **563** 410–418 (*Preprint* `astro-ph/0108227`)

[6] Howe R, Komm R W, Hill F, Haber D A and Hindman B W 2004 *Astrophys. J.* **608** 562–579

[7] Howe R, Komm R W and Hill F 2002 *Astrophys. J.* **580** 1172–1187

[8] Libbrecht K G and Woodard M F 1990 *Nat.* **345** 779–782

[9] Elsworth Y, Howe R, Isaak G R, McLeod C P, Miller B A, New R, Speake C C and Wheeler S J 1994 *Astrophys. J.* **434** 801–806

[10] Komm R, Howe R and Hill F 2002 *Astrophys. J.* **572** 663–673

[11] Jain R and Haber D 2002 *Astron. Astrophys.* **387** 1092–1099

[12] Howe R, Jain K, Bogart R S, Haber D A and Baldner C S 2012 *Solar Phys.* **281** 533–549 (*Preprint* `1208.1644`)